



ELSEVIER

Available online at [www.sciencedirect.com](http://www.sciencedirect.com)

SCIENCE @ DIRECT®

Nuclear Physics A 761 (2005) 313–332

NUCLEAR  
PHYSICS A

# Extracting information on the $0\nu\beta\beta$ decays from the $2\nu\beta\beta$ decays

O. Civitarese<sup>a,\*</sup>, J. Suhonen<sup>b</sup>

<sup>a</sup> *Department of Physics, University of La Plata, CC 67, 1900-La Plata, Argentina*

<sup>b</sup> *Department of Physics, University of Jyväskylä, PO Box 35, FIN-40014, Jyväskylä, Finland*

Received 3 March 2005; received in revised form 8 July 2005; accepted 21 July 2005

Available online 15 August 2005

---

## Abstract

We have analyzed the relation between the two-neutrino ( $2\nu\beta\beta$ ) and neutrinoless ( $0\nu\beta\beta$ ) double beta decays of  $^{76}\text{Ge}$ ,  $^{82}\text{Se}$ ,  $^{100}\text{Mo}$ , and  $^{116}\text{Cd}$ . The relevant nuclear matrix elements have been calculated by using the proton–neutron quasiparticle random-phase approximation (pn-QRPA) with realistic two-body interactions. The dependence of the calculated matrix elements on the strength  $g_{pp}$  of the particle–particle part of the proton–neutron two-body interaction is investigated. Recently a procedure was proposed where data on  $2\nu\beta\beta$ -decay half-lives could be used to derive appropriate values of  $g_{pp}$  for calculating the  $0\nu\beta\beta$ -decay matrix elements. Following this procedure, we have determined the allowed values of  $g_{pp}$  by including experimental errors of the measured  $2\nu\beta\beta$ -decay half-lives and the uncertainties in the axial-vector coupling constant  $g_A$ . This set of  $g_{pp}$  values is used to predict single-beta and  $0\nu\beta\beta$  observables. Careful study of these observables points to serious shortcomings in the adopted procedure.

© 2005 Elsevier B.V. All rights reserved.

PACS: 14.60.Pq; 23.40.Bw; 23.40.Hc

Keywords: Double beta decay; Quasiparticle random-phase approximation; Nuclear matrix elements; Multipole decomposition

---

\* Corresponding author.

E-mail address: [civitare@fisica.unlp.edu.ar](mailto:civitare@fisica.unlp.edu.ar) (O. Civitarese).

## 1. Introduction

The amount of data acquired in recent neutrino-oscillation experiments [1] allow for a well founded description of neutrino properties in terms of oscillations between neutrino mass eigenstates. The present status of the components of the neutrino mixing matrix has been reported in [2,3]. Also, recent studies have shown that the possible scenarios concerning light-neutrino masses may be those where the mass eigenvalues are arranged hierarchically [2]. The absolute scale of the neutrino mass is still beyond the reach of the present experiments. At the moment the most feasible way to determine the mass scale is by the observation of neutrinoless double beta decay.

Double beta decay processes are indeed the unique tool to extract this information [3–6]. However, since the physics of double beta decay necessarily refers to the knowledge of nuclear-structure properties, precise determination of the neutrino mass from the half-life data is strongly hampered by the uncertainties in the calculated nuclear matrix elements [6]. The problem of fixing the nuclear-model parameters, and particularly the strength of the attractive proton–neutron interaction in the  $1^+$  channel, scaled by the parameter  $g_{pp}$  [7,8], has captured the attention of nuclear physicist for almost 20 years [6]. This issue is very important due to the observed [7,8] strong dependence of the value of the  $2\nu\beta\beta$  nuclear matrix element on  $g_{pp}$ , sometimes called the  $g_{pp}$  problem of the  $2\nu\beta\beta$  decay. Further details about the nuclear-structure models and approximations, involved in the microscopic description of both the two-neutrino and neutrinoless modes of double beta decay can be found in, e.g., [6].

In [6] we have advocated in favor of a case-by-case analysis of the nuclear systems where double beta decay can occur. We have focussed our attention on adequate theoretical description of spectroscopic observables, including lateral  $\beta^-$ -decay and electron-capture feeding of nuclear states in the even–even mother and daughter nuclei of double beta decay (see, e.g., [9,10]). In addition, the effects of the size of single-particle valence space [11] and the sequence of individual single-quasiparticle levels for odd-mass nuclei in the neighborhood of the participant double beta decay nuclei has been addressed [12]. Lately, the connection between the  $\beta$ -decay and  $2\nu\beta\beta$ -decay matrix elements was studied in [13].

A different approach to the problem was suggested in a recent publication [14]. Therein, a procedure to limit the theoretical uncertainties which affect the estimates of  $0\nu\beta\beta$  matrix elements was advocated and applied to some of the  $\beta\beta$  decay emitters. The procedure presented in [14] may be summarized as the following steps:

- (a) The strength of the particle–particle part of the proton–neutron interaction,  $g_{pp}$ , is fixed by reproducing the experimental nuclear matrix elements extracted from the measured  $2\nu\beta\beta$ -decay half-lives, and
- (b) this very value of  $g_{pp}$  is used to calculate the nuclear matrix elements relevant for  $0\nu\beta\beta$  decay.

The steps (a) and (b) were applied in [14] to various microscopic two-body interactions which, in turn, were approximately diagonalized using the standard proton–neutron quasiparticle random-phase approximation (pn-QRPA) [8] and also its renormalized version

(pn-RQRPA) [17]. From their results the authors of [14] claimed that their procedure is able to produce reliable nuclear matrix elements which exhibit a certain degree of independence with respect to the interaction as well as to the method, pn-QRPA or pn-RQRPA, used to solve the many-body problem. These are very interesting results, indeed, the validity of which needs to be verified in a systematic manner. Since we focus our attention on the specific question about the possible relation between two-neutrino and neutrinoless-double beta decay matrix elements, we shall not review here the indeed vast existing literature which deals with the more general subject of the theoretical approaches which may be applied to describe nuclear double beta decay transitions. We leave this for the reader, with the help of references [3–6]. As we have pointed out before, we shall concentrate on the use of the conventional pn-QRPA approach [8]. For extensions of this method, and related ones, the reader may consult Refs. [3–6].

Double beta decay studies have been performed in other approaches, like the shell model, see, i.e., [15]. The progress achieved during the last decade in shell model calculations is considerable [16]. However, the difficulties posed by the formidable task of dealing with realistic interactions in huge basis persist and we are still forced to use approximations, like the pn-QRPA, to perform systematic studies of these transitions. As said before in this work we focus on the RPA-type of approaches.

In this paper we have taken the results of [14] as our main motivation and we have adopted a similar starting point, that is the adjustment of the parameter  $g_{pp}$  to reproduce the  $2\nu\beta\beta$ -decay data. We have improved the method of [14] by including experimental errors of the data. We have also included the uncertainties stemming from the adopted value of the axial-vector coupling constant,  $g_A$ . The effective value of this coupling constant is not known in finite nuclei of medium-heavy and heavy masses. Our adopted effective values of  $g_A$ , between  $g_A = 1.0$ – $1.25$ , simulate the nuclear many-body effects on the involved spin–isospin dependent operators. The quenched values of  $g_A$  are a simplified means of renormalizing these operators for calculations performed in finite valence spaces. The origin of the quenching of  $g_A$  can also be a more general property of the nuclear medium but this issue has not been settled yet. In any case, we include the possible variation in the effective value of  $g_A$  without trying to resolve its fundamental origin.

The experimental errors and the uncertainty in  $g_A$  produce an interval of allowed values of the extracted  $2\nu\beta\beta$ -decay matrix elements. This, in turn, leads to an interval for the fitted values of  $g_{pp}$ . Within this interval we have investigated the dependence on  $g_{pp}$  of the magnitude and decomposition of the  $0\nu\beta\beta$  matrix elements. In particular, we have addressed the role and relevance of the  $1^+$  channel, relative to other involved multipoles, in this decomposition. In these studies we analyze the feasibility of the method advocated in [14].

Our article is organized as follows: in Section 2 we present the essential ingredients of the  $2\nu\beta\beta$ -decay and  $0\nu\beta\beta$ -decay formalisms, needed to follow our discussion of the results. In Section 3 we present the results and discuss them from the viewpoints of single beta decays and double beta decays. Finally, in Section 4 we draw conclusions of our studies.

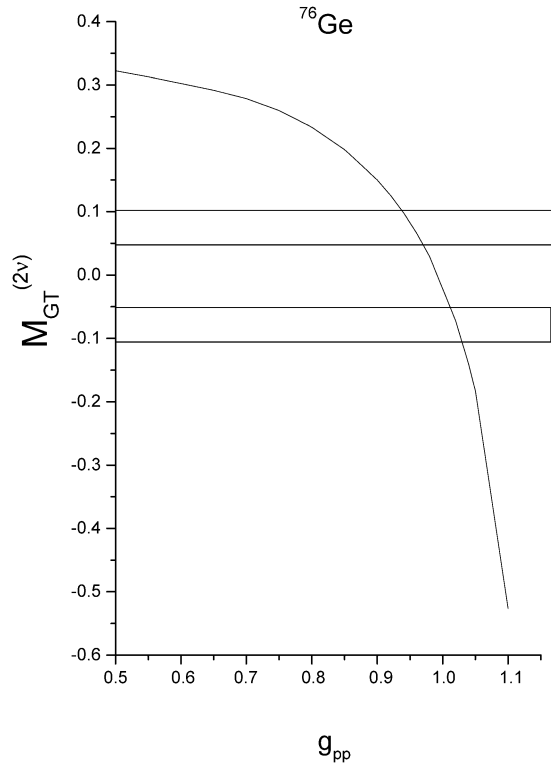


Fig. 1. Dependence of the computed matrix element  $M_{GT}^{(2\nu)}$  on  $g_{pp}$  for the decay of  $^{76}\text{Ge}$ . The boxes enclose the values of  $2\nu\beta\beta$  matrix elements extracted from measurements of the decay half-life, including experimental error bars. The intersections with the theoretical results (solid line) indicate the ranges of  $g_{pp}$  values where the computed matrix element is compatible with the data.

## 2. Formalism

In this section we briefly introduce the formalism which we have used to obtain the computed results for the  $2\nu\beta\beta$  and  $0\nu\beta\beta$  observables. We start by writing down an expression for the  $2\nu\beta\beta$ -decay half-life,  $t_{1/2}^{(2\nu)}$  for transition from the initial ground state,  $0_I^+$  to the final ground state,  $0_F^+$ . This expression reads

$$[t_{1/2}^{(2\nu)}(0_I^+ \rightarrow 0_F^+)]^{-1} = G^{(2\nu)} |M_{GT}^{(2\nu)}|^2, \tag{1}$$

where  $G^{(2\nu)}$  is an integral over the phase space of the leptonic variables [6].

The nuclear two-body Gamow–Teller matrix element,  $M_{GT}^{(2\nu)}$ , corresponding to the  $2\nu\beta\beta$  decay, can be written as

$$M_{GT}^{(2\nu)} = \sum_{m,n} \frac{\langle 0_F^+ || \sum_j \sigma(j) t_j^- || 1_n^+ \rangle \langle 1_n^+ | 1_m^+ \rangle \langle 1_m^+ || \sum_j \sigma(j) t_j^- || 0_I^+ \rangle}{(\frac{1}{2} Q_{\beta\beta} + E_n - M_I)/m_e + 1}, \tag{2}$$

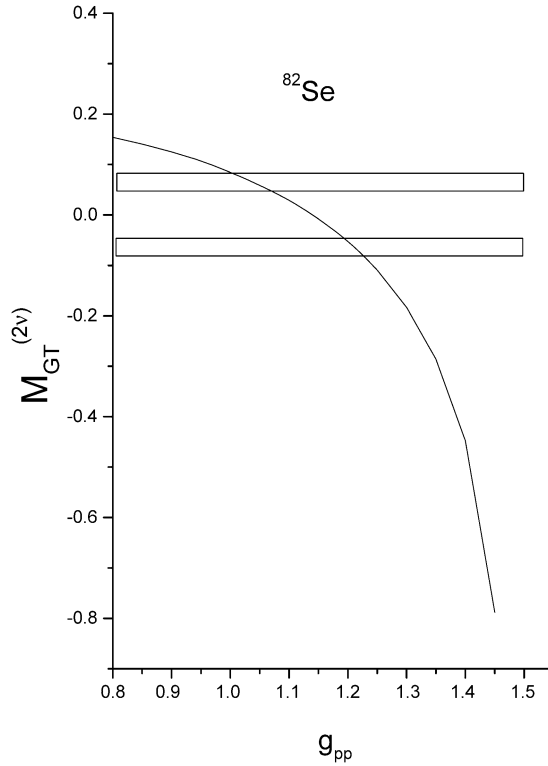


Fig. 2. The same as Fig. 1 for the  $2\nu\beta\beta$  decay of  $^{82}\text{Se}$ .

where the transition operators are the usual Gamow–Teller operators for  $\beta^-$  transitions,  $Q_{\beta\beta}$  is the  $2\nu\beta\beta$   $Q$  value,  $E_n$  is the energy of the  $n$ th intermediate state,  $M_I$  is the mass energy of the initial nucleus, and  $m_e$  is the rest-mass of the electron. The overlap  $\langle 1_n^+ | 1_m^+ \rangle$  takes into account the fact that within the pn-QRPA approach we have to generate the set of intermediate states by starting separately from the mother and daughter ground states. This yields two sets of intermediate states and the overlap is used to connect members of these sets.

In the extremely simple case, when only the lowest intermediate  $1^+$  state in (2) dominates, one can write  $M_{\text{GT}}^{(2\nu)}$  approximately as

$$M_{\text{GT}}^{(2\nu)} \cong \frac{M_{\text{EC}}M_{\beta^-}}{(\frac{1}{2}Q_{\beta\beta} + E_1 - M_I)/m_e + 1}. \quad (3)$$

In this case we have assumed that for a pn-QRPA calculation the overlap factor in (2) is roughly equals to one. This is indeed in practical calculations to within 20 percent. The situation shown in (3) is called the single-state dominance (SSD) and it was studied extensively in [18]. The two branches of the  $2\nu\beta\beta$  transition,  $M_{\text{EC}}$  and  $M_{\beta^-}$ , can in some cases be determined from experimental data. This is due to the fact that  $M_{\text{EC}}$  corresponds to electron-capture (EC) decay of the  $1_1^+$  state of the intermediate odd–odd nucleus to the

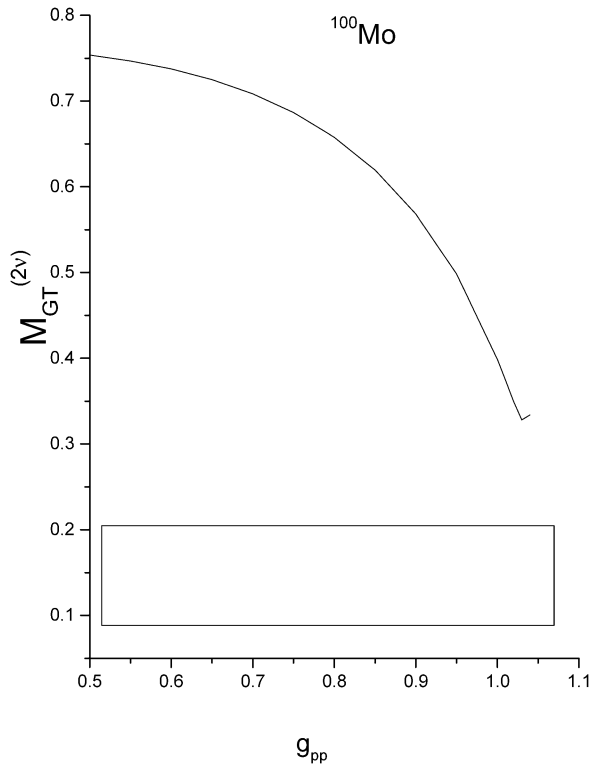


Fig. 3. The same as Fig. 1 for the  $2\nu\beta\beta$  decay of  $^{100}\text{Mo}$ .

initial even–even ground state of the  $2\nu\beta\beta$  transition. Furthermore,  $M_{\beta^-}$  corresponds to the  $\beta^-$  decay of the same state to the final even–even ground state of the  $2\nu\beta\beta$  transition. Sometimes data exists for half-lives of these two branches of  $1_1^+$ -state de-excitation.

Let us now turn to the case of the  $0\nu\beta\beta$  decays. The inverse half-life for  $0\nu\beta\beta$ -decay transitions, mediated by the neutrino mass, is written [6,19] as

$$[t_{1/2}^{(0\nu)}(0_I^+ \rightarrow 0_F^+)]^{-1} = C_{mm}^{(0\nu)} \left( \frac{\langle m_\nu \rangle}{m_e} \right)^2, \quad (4)$$

where  $0_I^+$  is the initial ground state and  $0_F^+$  the final one. Here  $\langle m_\nu \rangle$  is the effective neutrino mass being a linear combination of the mass eigenstates weighted by the elements of the neutrino mixing matrix [6,19]. Relation of this quantity to the neutrino-mass hierarchies and experimentally determined elements of the mixing matrix has been discussed, e.g., in [20,21]. In the present discussion we have omitted the possible contributions from right-handed currents [6,19] and supersymmetric particles [22].

Table 1

Data on  $2\nu\beta\beta$  decays. The double beta decay system is indicated in the first column. The calculated phase space factor,  $G^{(2\nu)}$  [yr] $^{-1}$ , is given in the second column. For each case the central value of the experimental half-life,  $t_{1/2}^{(2\nu)}$ , is given in the third column. The experimental errors are indicated by  $\Delta_+$  and  $\Delta_-$ , so that the data are expressed as  $t_{1/2,\text{exp}}^{(2\nu)} = t_{1/2-\Delta_-}^{(2\nu)+\Delta_+}$ . In the last column (r.v.) stands for the recommended value [26]. The rest of the experimental values are taken from [27] using the same notation for the original references

Case	$G^{(2\nu)}$ [yr] $^{-1}$	$t_{1/2}^{(2\nu)}$ [yr]	$\Delta_+$ [yr]	$\Delta_-$ [yr]	Refs.
$^{76}\text{Ge}$	$1.3 \times 10^{-19}$	$1.43 \times 10^{21}$	$0.9 \times 10^{20}$	$0.7 \times 10^{20}$	r.v.
		$9.0 \times 10^{20}$	$1.0 \times 10^{20}$	$1.0 \times 10^{20}$	Vas90a
		$1.1 \times 10^{21}$	$0.6 \times 10^{21}$	$0.3 \times 10^{21}$	Mil90
		$8.4 \times 10^{20}$	$1.0 \times 10^{20}$	$0.8 \times 10^{20}$	Bro93
		$1.1 \times 10^{21}$	$0.2 \times 10^{21}$	$0.2 \times 10^{21}$	Aal96
		$1.8 \times 10^{21}$	$0.1 \times 10^{21}$	$0.1 \times 10^{21}$	Gun97
$^{82}\text{Se}$	$4.3 \times 10^{-18}$	$0.96 \times 10^{20}$	$0.3 \times 10^{20}$	$0.1 \times 10^{20}$	r.v.
		$1.1 \times 10^{20}$	$0.3 \times 10^{20}$	$0.1 \times 10^{20}$	Ell92
		$8.3 \times 10^{19}$	$1.2 \times 10^{19}$	$1.2 \times 10^{19}$	Arn98
$^{100}\text{Mo}$	$8.9 \times 10^{-18}$	$8.0 \times 10^{18}$	$0.7 \times 10^{18}$	$0.7 \times 10^{18}$	r.v.
		$3.3 \times 10^{18}$	$2.0 \times 10^{18}$	$1.0 \times 10^{18}$	Vas90b
		$1.2 \times 10^{19}$	$0.5 \times 10^{19}$	$0.3 \times 10^{19}$	Ejj91
		$9.5 \times 10^{18}$	$1.0 \times 10^{18}$	$1.0 \times 10^{18}$	Das95
		$7.6 \times 10^{18}$	$2.2 \times 10^{18}$	$1.4 \times 10^{18}$	Als97
		$6.8 \times 10^{18}$	$0.8 \times 10^{18}$	$0.9 \times 10^{18}$	Sil97
$^{116}\text{Cd}$	$7.4 \times 10^{-18}$	$3.3 \times 10^{19}$	$0.3 \times 10^{19}$	$0.3 \times 10^{19}$	r.v.
		$2.6 \times 10^{19}$	$0.9 \times 10^{19}$	$0.5 \times 10^{19}$	Ejj95
		$2.7 \times 10^{19}$	$1.0 \times 10^{19}$	$0.7 \times 10^{19}$	Dan95
		$3.8 \times 10^{19}$	$0.4 \times 10^{19}$	$0.4 \times 10^{19}$	Arn96
		$2.6 \times 10^{19}$	$0.7 \times 10^{19}$	$0.4 \times 10^{19}$	Dan00

From the point of view of the present discussion the relevant ingredients are contained in the factor  $C_{mm}^{(0\nu)}$  of (4). This factor contains the leptonic phase space and the nuclear structure in the form

$$C_{mm}^{(0\nu)} = G_1^{(0\nu)} (M_{\text{GT}}^{(0\nu)} (1 - \chi_{\text{F}}))^2, \quad \chi_{\text{F}} = \left( \frac{g_{\text{V}}}{g_{\text{A}}} \right)^2 \frac{M_{\text{F}}^{(0\nu)}}{M_{\text{GT}}^{(0\nu)}}, \quad (5)$$

where  $G_1^{(0\nu)}$  is the leptonic phase-space part and

$$M_{\text{GT}}^{(0\nu)} = (m_{\text{e}}R)^{-2} \sum_{ij} \sum_a \langle 0_{\text{F}}^+ || h_+(r_{ij}, E_a) \sigma(i) \sigma(j) \tau(i)^- \tau(j)^- || 0_{\text{I}}^+ \rangle \quad (6)$$

is the nuclear matrix element of the two-body Gamow–Teller operator. It should be noted that in the above definition [23] we use the scaling factor  $(m_{\text{e}}R)^{-2}$  relative to the one introduced in [19]. The factor  $\chi_{\text{F}}$  is the ratio between the Fermi

$$M_{\text{F}}^{(0\nu)} = (m_{\text{e}}R)^{-2} \sum_{ij} \sum_a \langle 0_{\text{F}}^+ || h_+(r_{ij}, E_a) \tau(i)^- \tau(j)^- || 0_{\text{I}}^+ \rangle \quad (7)$$

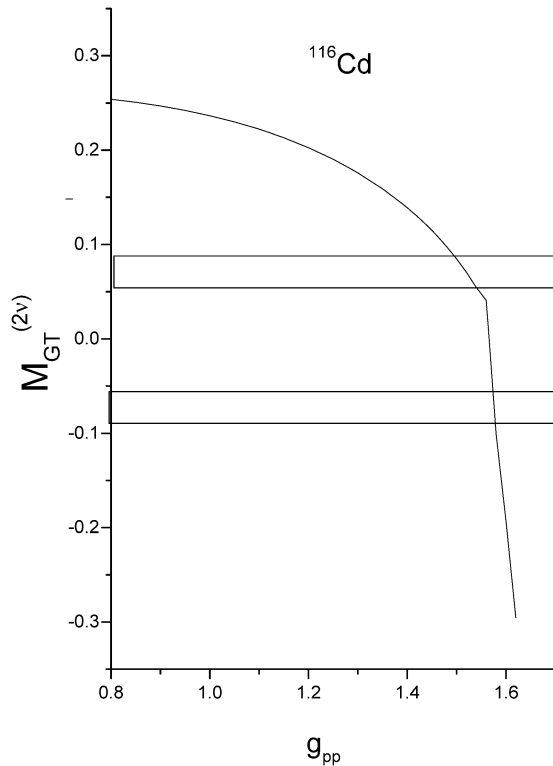


Fig. 4. The same as Fig. 1 for the  $2\nu\beta\beta$  decay of  $^{116}\text{Cd}$ .

and the Gamow–Teller matrix element (6). The axial-vector coupling constant  $g_A$  has been absorbed into the definition of the phase-space integral  $G_1^{(0\nu)}$  [6,19] and into the ratio  $\chi_F$ .

The matrix element (6) is evaluated by expanding the neutrino potential  $h_+(r_{ij})$  in spherical multipoles, which are then coupled to the spin operators appearing in (6). A suitable way to calculate this expansion consists of introducing, for each multipole, a complete set of states labelled by the quantum numbers  $a$  in (6). These are nuclear states whose wave functions should be determined to compute the transition amplitudes [6].

### 3. Results and discussion

#### 3.1. Parameters of the Hamiltonian

The calculation of the matrix elements (2) and (6) proceeds as follows. The single-particle energies of the spherical mean field are obtained from a Woods–Saxon single-particle potential, including the Coulomb and spin–orbit parts in the Bohr–Mottelson parametrization [24]. The single-particle valence space is taken typically to span two to three oscillator major shells around the proton and neutron Fermi surfaces in a way described in

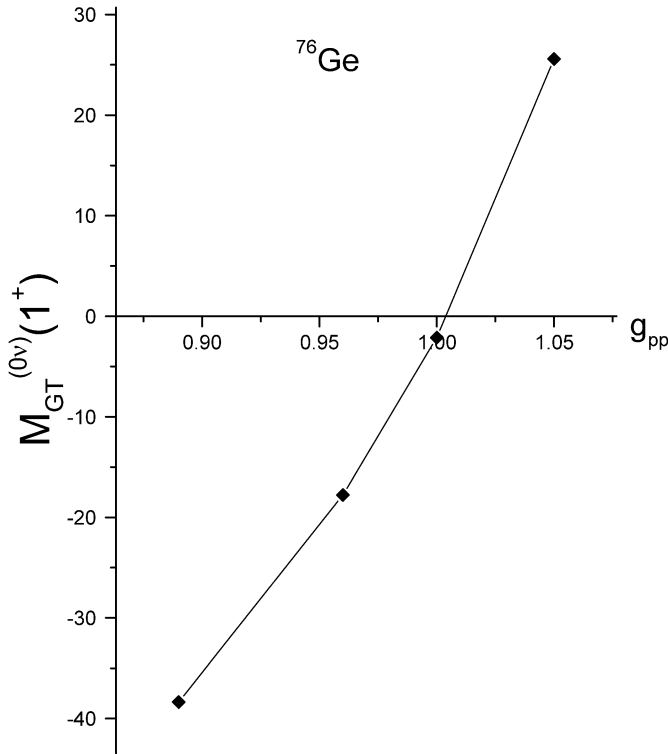


Fig. 5. Dependence of the matrix element  $M_{GT}^{(0\nu)}(1^+)$  on  $g_{pp}$  for the  $0\nu\beta\beta$  decay of  $^{76}\text{Ge}$ . Notice that the sign is irrelevant, since only one set of states (the set of  $1^+$  states) was included in the calculations.

[18]. The adopted two-body interaction is a realistic one, based on the one-boson-exchange potential of the Bonn type, transformed to nuclear matter by the G-matrix technique. The finite-size effects have been taken into account in an approximate way by using simple scaling parameters both for the short-range and long-range parts of the two-body interaction in its particle–hole and particle–particle channels. This scaling is discussed below.

The strong short-range correlations between nucleons have been treated by using the BCS approximation. The associated pairing strengths are adjusted to reproduce the empirical pairing gaps, extracted from the experimental separation energies of protons and neutrons, in a way described in [25]. The many-body aspects of the problem were handled by the use of the pn-QRPA. In the case of the beta decays and  $2\nu\beta\beta$  decays the involved multipole of the odd–odd intermediate nucleus is  $J^\pi = 1^+$ . In this case the proton–neutron correlations are treated by fixing the scale of the particle–hole two-body matrix elements to reproduce the empirical location of the Gamow–Teller giant resonance. The particle–particle part of the same interaction is scaled by the interaction strength constant  $g_{pp}$  which is adjusted using the data on  $2\nu\beta\beta$ -decay half-lives. For the other multipoles, appearing in the  $0\nu\beta\beta$  matrix element (6), the particle–hole channel was kept as a bare G-matrix and the particle–particle channel was scaled by the value of  $g_{pp}$  extracted from the  $J^\pi = 1^+$  multipole.

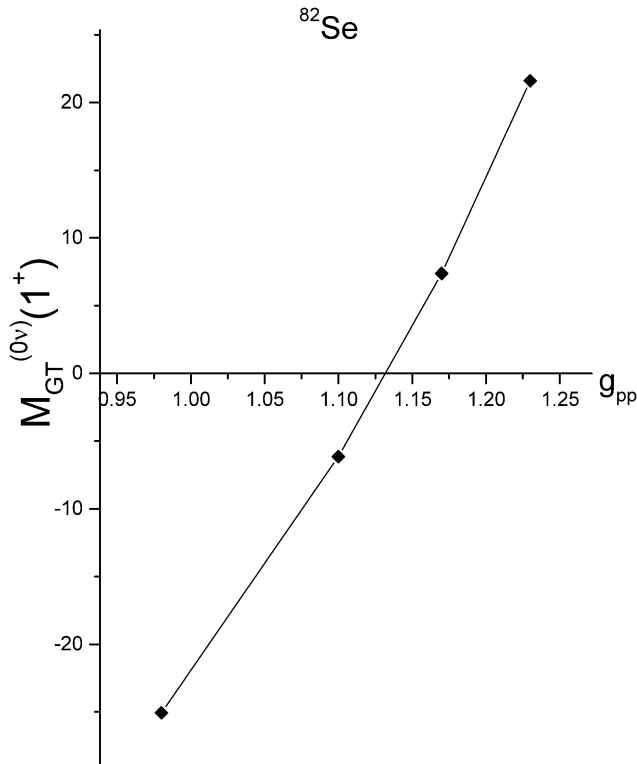


Fig. 6. The same as Fig. 5 for the  $0\nu\beta\beta$  decay of  $^{82}\text{Se}$ .

### 3.2. Single beta decay

Let us first briefly discuss the effect on single beta decays of the fixing of  $g_{pp}$  by the  $2\nu\beta\beta$ -decay data. In [13] it was found that by fixing  $g_{pp}$  by the  $2\nu\beta\beta$ -decay data the resulting computed  $\beta^-$  and EC matrix elements,  $M_{\beta^-}$  and  $M_{EC}$  in Eq. (3), fail to reproduce the corresponding data. In [13] this was studied for the nuclei  $^{76}\text{Ge}$ ,  $^{82}\text{Se}$ ,  $^{100}\text{Mo}$ ,  $^{116}\text{Cd}$ , and  $^{128}\text{Te}$ . The mechanism behind this is easy to grasp when considering the  $2\nu\beta\beta$  decay in the SSD approximation (3). For, e.g.,  $^{100}\text{Mo}$  and  $^{116}\text{Cd}$  this seems to be a reasonable approximation. One first uses the  $2\nu\beta\beta$ -decay data to fix  $g_{pp}$ . The matrix element  $M_{EC}$ , computed for this value of  $g_{pp}$ , produces a far too large decay rate for the corresponding EC transition as compared to experimental data. At the same time the computed  $M_{\beta^-}$ , for the same  $g_{pp}$  value, produces a far too small decay rate for the corresponding  $\beta^-$  transition. Hence, use of this extracted value of  $g_{pp}$  reproduces the  $2\nu\beta\beta$  half-life via two compensating errors: too large an EC matrix element is compensated by too small a  $\beta^-$  matrix element.

In [13] it was advocated that a more proper determination of the value of the  $g_{pp}$  parameter could be done by using experimental information on the  $\beta^-$  decay half-life. This procedure can lead to a notably different value of  $g_{pp}$  from the one extracted by using the  $2\nu\beta\beta$  decay half-life, even in the simple case of the SSD. In [13] it was noticed that

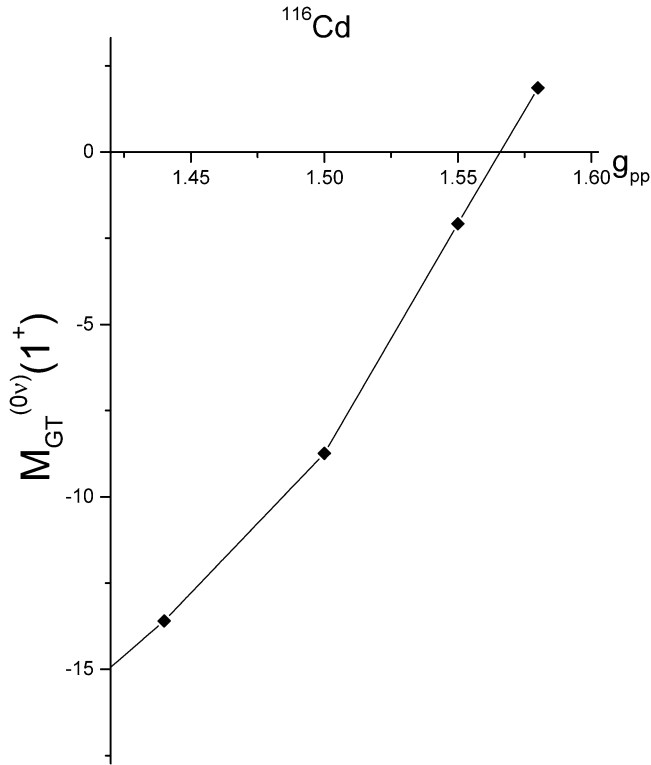


Fig. 7. The same as Fig. 5 for the  $0\nu\beta\beta$  decay of  $^{116}\text{Cd}$ .

the value of  $g_{pp}$ , extracted from the  $\beta^-$  data, could reproduce both the EC-decay and the  $\beta^-$ -decay data rather well for most of the cases.

### 3.3. Two-neutrino double beta decay

To begin with the discussion of our results we show, in Figs. 1–4, the calculated matrix elements  $M_{GT}^{(2\nu)}$  of (2) for all the considered  $2\nu\beta\beta$  transitions. To extract the experimental values we have used the recommended values for the half-lives [26] in combination with the ones reported in [27], adding also the experimental errors. The used data is summarized in Table 1.

Then we have extracted the largest and smallest values of  $M_{GT}^{(2\nu)}$  allowed by the data. In doing this we have used the range  $g_A = 1.0$ – $1.254$  for the values of the axial-vector coupling constant. The horizontal limits in Figs. 1–4 indicate the range of  $M_{GT}^{(2\nu)}$  deduced by using this method. The intersections of these lines and the curves representing the corresponding theoretical values determine, for each case, the allowed values of  $g_{pp}$ . One should note here that we have allowed both positive and negative values of the matrix elements compatible with the data. This results in two symmetrical stripes of allowed experimental matrix elements yielding two ranges of possible  $g_{pp}$  values.

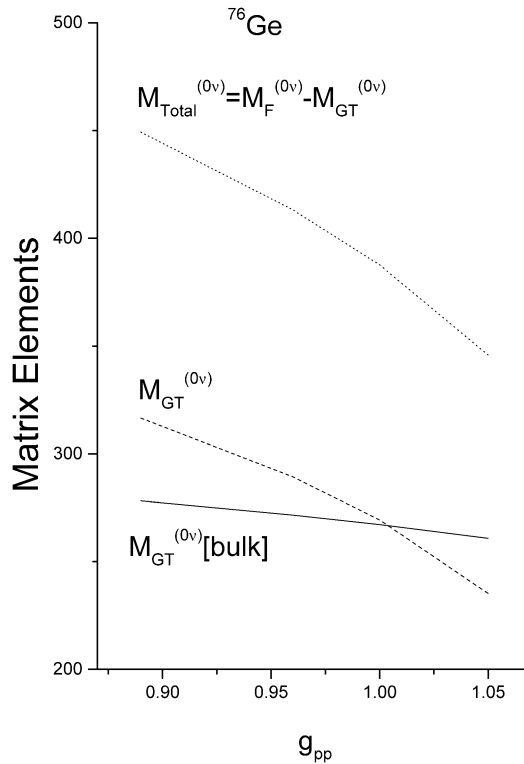


Fig. 8. Dependence of the two-body Gamow–Teller matrix element on the parameter  $g_{\text{pp}}$  for the  $0\nu\beta\beta$  decay of  $^{76}\text{Ge}$ . The values indicated by  $M_{\text{GT}}(\text{bulk})$  contain the contributions of all multipoles except  $J^\pi = 1^+$ . The values denoted by  $M_{\text{GT}}$  are the ones which included the contribution of  $J^\pi = 1^+$ . The matrix element  $M_{\text{Total}}$  is the sum of the Gamow–Teller and Fermi contributions.

The cases of  $^{76}\text{Ge}$  and  $^{82}\text{Se}$  in Figs. 1 and 2 are examples of a situation where the region where the pn-QRPA collapses is far from the region where the matrix element  $M_{\text{GT}}^{(2\nu)}$  is suppressed to its experimental value by the renormalization of particle–particle correlations. In the case of  $^{100}\text{Mo}$ , in Fig. 3,  $M_{\text{GT}}^{(2\nu)}$  is not totally suppressed and its values reaches a minimum, without touching the region allowed by the data. For this case we have taken only the value of  $g_{\text{pp}}$  corresponding to the minimum of  $M_{\text{GT}}^{(2\nu)}$ . The peculiar behavior of  $M_{\text{GT}}^{(0\nu)}$  for  $^{100}\text{Mo}$  stems from the adopted single-particle energies which we have computed by using the standard parameters of the Woods–Saxon potential described previously. Similar behavior was reported in [29] for the case of  $^{106}\text{Cd}$ . There a modification of the spin–orbit force was used to obtain a more smooth behavior of the  $2\nu\beta\beta$ -decay matrix element. One could also resort to the experimentally available single-particle energies, as was done in [30]. Here we are not using the  $2\nu\beta\beta$ -decay matrix element to obtain the  $0\nu\beta\beta$ -decay matrix element and thus we do not need to modify our single-particle energies to be able to fit the experimental  $2\nu\beta\beta$ -decay rate.

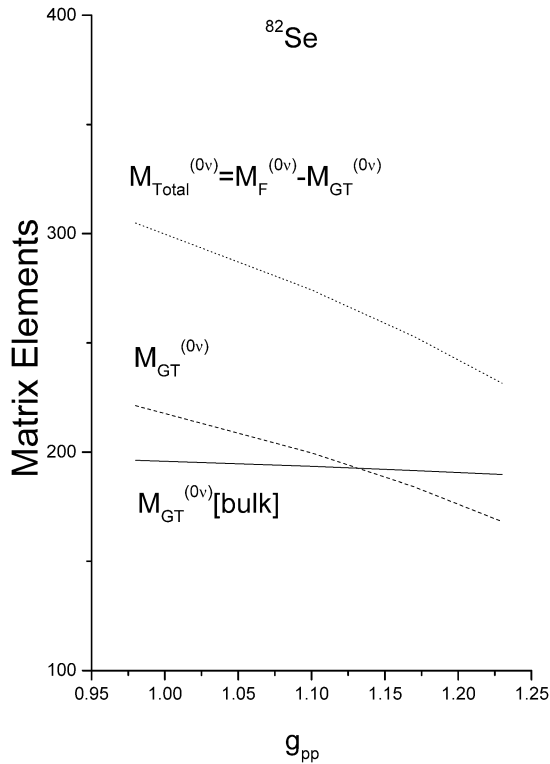


Fig. 9. The same as Fig. 8 for the  $0\nu\beta\beta$  decay of  $^{82}\text{Se}$ .

The case of  $^{116}\text{Cd}$  illustrates a situation where the point of collapse is close to the point of total suppression of  $M_{\text{GT}}^{(2\nu)}$ . Hence, in the region of allowed values of  $M_{\text{GT}}^{(2\nu)}$  the value of the computed matrix element changes very fast leading to small allowed ranges for  $g_{\text{pp}}$ .

From this first set of results we may conclude that by including the experimental errors of the measured half-lives and the uncertainties in the value of  $g_A$  produces not only one value but a *range* of values for  $g_{\text{pp}}$  by the procedure suggested in [14]. Naturally, this is not necessarily a drawback of the procedure, since we still have to assess the consequences of it upon the determination of the values of the matrix elements  $M_{\text{GT}}^{(0\nu)}$ .

### 3.4. Neutrinoless double beta decay

The nuclear matrix element governing the mass sector of the  $0\nu\beta\beta$  decay mode, see Eqs. (4)–(6), has two contributions, namely the ones due to Gamow–Teller and Fermi transitions. The Gamow–Teller part of the matrix element,  $M_{\text{GT}}^{(0\nu)}$ , is the more important one and collects also the contributions coming from  $J^\pi = 1^+$  virtual transitions. We are thus tempted to see if this contribution shows the trend exhibited by the matrix element for the two-neutrino case, where the  $1^+$  is the only allowed channel.

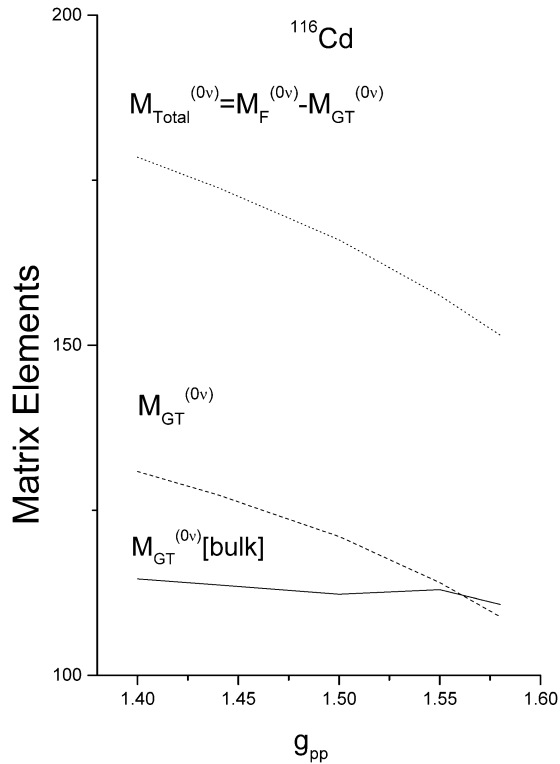


Fig. 10. The same as Fig. 8 for the  $0\nu\beta\beta$  decay of  $^{116}\text{Cd}$ .

Figs. 5–7 show the dependence of  $M_{\text{GT}}^{(0\nu)}(1^+)$ , that is the contribution of the  $1^+$  set of states to  $M_{\text{GT}}^{(0\nu)}$ , for the values of  $g_{\text{pp}}$  determined previously (see Figs. 1–4). The case of  $^{100}\text{Mo}$  has been omitted because for it only one value of  $g_{\text{pp}}$  is taken, as explained before. As can be seen from Figs. 5–7, the  $1^+$  contributions the  $0\nu\beta\beta$  transitions exhibit a similar pattern to the one shown in Figs. 1–4 for the  $2\nu\beta\beta$  transitions. It means that in the neutrinoless mode, just like in the two-neutrino mode, the contribution of the set of  $1^+$  states is suppressed by the proton–neutron particle–particle interactions.

Bearing in mind that all the other multipoles, with angular momenta  $J = 2, 3, 4, \dots$  and both parities, contribute to  $M_{\text{GT}}^{(0\nu)}$  one may wonder how the changes in  $g_{\text{pp}}$  influence the total matrix element: is it suppressed and how much? To answer this question we have calculated separately the value of  $M_{\text{GT}}^{(0\nu)}$ , with and without the contribution of the  $1^+$  states. The results are shown in Figs. 8–10. There  $M_{\text{GT}}(\text{bulk})$  represents the matrix element  $M_{\text{GT}}^{(0\nu)}$  without the contribution from the  $1^+$  states, while  $M_{\text{GT}}$  has their contribution included. These figures do not show the case of  $^{100}\text{Mo}$  since for it no  $g_{\text{pp}}$  interval is obtained from the analysis of the  $2\nu\beta\beta$ -decay matrix element.

From the figures it is obvious that  $M_{\text{GT}}(\text{bulk})$  is practically constant over the allowed range of values of  $g_{\text{pp}}$ . This means that in the region of values of  $g_{\text{pp}}$ , determined by using the procedure of [14], the effect of this parameter on the relevant matrix element, that is the

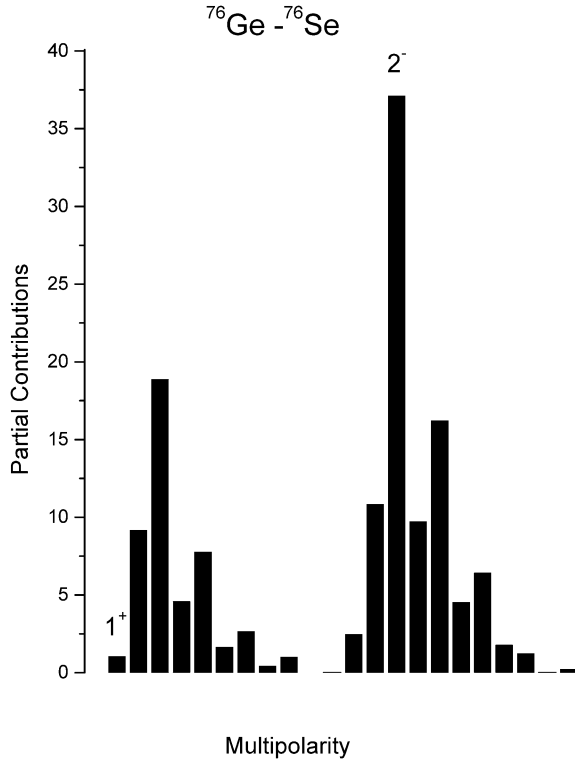


Fig. 11. Multipole decomposition of the matrix element  $M_{GT}^{(0v)}$  for the decay of  $^{76}\text{Ge}$ . The values shown in the figure have been obtained with  $g_{pp} = 1.0$ . The contributions of the multipoles with positive parity read from left ( $J^\pi = 1^+$ ) to right ( $J^\pi = 9^+$ ), while the negative parities read from left ( $J^\pi = 10^-$ ) to right ( $J^\pi = 20^-$ ). For the sake of comparison we have indicated, explicitly, the contributions of the  $1^+$  and  $2^-$  set of states.

bulk one, is practically null. Considering the values of the total matrix element  $M_{GT}^{(0v)}$ , denoted by  $M_{\text{total}}$  in Figs. 8–10, it is seen that the changes are of the order of 10 to 20 percent within the allowed ranges of  $g_{pp}$ . This small variation stems from the above discussed very small variation of  $M_{GT}(\text{bulk})$  and the fact that within the allowed region the  $1^+$  contribution lies close to its complete cancellation and the variations of it with  $g_{pp}$  do not affect much the total matrix element. In other words, the  $1^+$  contribution is efficiently damped by the contributions coming from the other multipoles which are practically independent of  $g_{pp}$  in its allowed region. In Table 2 numerical values corresponding to Figs. 8–10 are shown to gain a quantitative estimate of the effect.

The allowed ranges of the matrix elements  $M_{GT}^{(0v)}$  are reflected in the values of the  $C_{mm}^{(0v)}$  coefficients in Eq. (5). The  $g_{pp}$  and  $g_A$  dependence of these coefficients is documented in Table 3. There the values of the  $C_{mm}^{(0v)}$  coefficients are given for the two extreme values of  $g_A$  and for the four  $g_{pp}$  values at the borders of the allowed ranges. As mentioned before,  $^{100}\text{Mo}$  is an exception since for it only one  $g_{pp}$  value is used. Table 3 shows that the inclusion of experimental errors in the  $2\nu\beta\beta$  half-lives causes large variations in the calculated values of  $C_{mm}^{(0v)}$ . The changes in  $g_A$  induce changes of  $C_{mm}^{(0v)}$  by a factor  $\approx 2$ .

Table 2

Value of the matrix element  $M_{GT}^{(0\nu)}$  of Eq. (5) as a function of the parameter  $g_{pp}$  across the domains of  $g_{pp}$  which best fit the experimental data on  $2\nu\beta\beta$ . The results of the sum over all multipoles is given in the third column, the contribution of only one set of states ( $J^\pi = 1^+$ ) is shown in the fourth column, and the bulk value, obtained by excluding the  $J^\pi = 1^+$  states from the sum, is shown in the fifth column. The last two columns show the results of the ratio  $\chi_F$ , for two values of the axial-vector coupling constant  $g_A = 1.00$  and  $g_A = 1.254$ , respectively

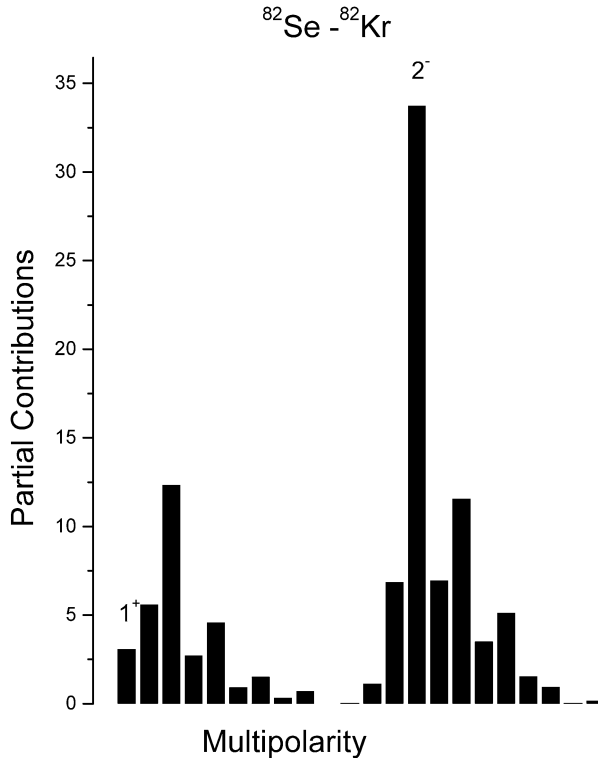
Case	$g_{pp}$	$M_{GT}^{(0\nu)}$ (all)	$M_{GT}^{(0\nu)}$ ( $1^+$ )	$M_{GT}^{(0\nu)}$ (bulk)	$\chi_F$ ( $g_A = 100$ )	$\chi_F$ ( $g_A = 1.254$ )
$^{76}\text{Ge}$	0.89	162.35	19.18	143.17	-0.419	-0.266
	0.96	148.31	8.89	139.42	-0.428	-0.272
	1.00	137.98	1.06	136.92	-0.439	-0.279
	1.05	120.39	-12.79	133.18	-0.470	-0.299
$^{82}\text{Se}$	0.98	114.83	12.23	102.60	-0.378	-0.240
	1.10	103.39	3.07	100.32	-0.374	-0.238
	1.17	95.16	-3.69	98.85	-0.374	-0.238
	1.23	86.70	-10.82	97.51	-0.376	-0.239
$^{100}\text{Mo}$	1.16	142.30	20.44	121.86	-0.373	-0.237
$^{116}\text{Cd}$	1.44	66.12	6.80	59.32	-0.363	-0.231
	1.50	62.77	4.37	58.40	-0.371	-0.236
	1.55	59.06	1.55	57.51	-0.381	-0.242
	1.58	56.01	-0.98	57.99	-0.391	-0.249

Table 3

Values of the coefficient  $C_{mm}^{(0\nu)}$  of Eq. (5), in units of  $\text{yr}^{-1}$ , for the  $g_{pp}$  and  $g_A$  values specified in the second and last two columns, respectively

Case	$g_{pp}$	$C_{mm}^{(0\nu)}$ ( $g_A = 1.00$ )	$C_{mm}^{(0\nu)}$ ( $g_A = 1.254$ )
$^{76}\text{Ge}$	0.89	$8.9492 \times 10^{-14}$	$1.7627 \times 10^{-13}$
	0.96	$7.5726 \times 10^{-14}$	$1.4860 \times 10^{-13}$
	1.00	$6.6630 \times 10^{-14}$	$1.3017 \times 10^{-13}$
	1.05	$5.3048 \times 10^{-14}$	$1.0239 \times 10^{-13}$
$^{82}\text{Se}$	0.98	$1.8752 \times 10^{-13}$	$3.7575 \times 10^{-13}$
	1.10	$1.5181 \times 10^{-13}$	$3.0469 \times 10^{-13}$
	1.17	$1.2908 \times 10^{-13}$	$2.5910 \times 10^{-13}$
	1.23	$1.0815 \times 10^{-13}$	$2.1683 \times 10^{-13}$
$^{100}\text{Mo}$	1.16	$5.2248 \times 10^{-13}$	$1.0493 \times 10^{-12}$
$^{116}\text{Cd}$	1.44	$1.3177 \times 10^{-13}$	$2.6542 \times 10^{-13}$
	1.50	$1.2005 \times 10^{-13}$	$2.4122 \times 10^{-13}$
	1.55	$1.0818 \times 10^{-13}$	$2.1645 \times 10^{-13}$
	1.58	$1.0008 \times 10^{-13}$	$1.9937 \times 10^{-13}$

The above results point to the conclusion that the choice of  $g_{pp}$ , advocated in [14], may lead to contradicting results for the single beta decays and does not affect much the total matrix elements of the  $0\nu\beta\beta$  decays. The effect of  $g_{pp}$  is seen in the contribution of the  $1^+$  multipole to  $M_{GT}^{(0\nu)}$  but not in the bulk of  $M_{GT}^{(0\nu)}$ . To investigate this aspect of the problem more carefully we have analyzed the multipole decomposition of  $M_{GT}^{(0\nu)}$  within the allowed intervals of  $g_{pp}$ . We have chosen a  $g_{pp}$  value which roughly reproduces the centroid of



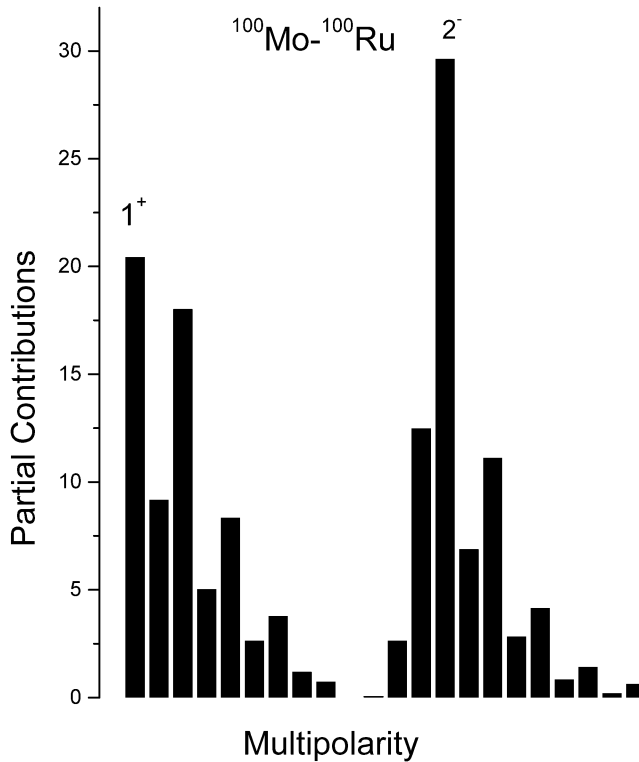


Fig. 13. Multipole decomposition of the matrix element  $M_{GT}^{(0\nu)}$  for the decay of  $^{100}\text{Mo}$ . The values shown in the figure have been obtained with  $g_{pp} = 1.05$ .

(a) they are almost insensitive to the type of microscopic two-body interaction used in the calculations, and

(b) the results are also very much independent of the pn-QRPA variant used to approximately diagonalize the proton–neutron interactions.

These are, in our opinion, important results, since they point out to a relative independence of the nuclear-structure component of the  $0\nu\beta\beta$ -decay problem on some of the essential elements entering the calculations. At this point it is worth pointing out that this independence has been discussed only for the QRPA-based class of models.

However, as we have shown in the previous section, the method of [14] cannot be considered as solution to the  $g_{pp}$  problem of double beta decay. The contradicting arguments can be condensed in the following:

(a) As shown explicitly in [13] the use of  $2\nu\beta\beta$ -decay transitions as a way to select the proper values of  $g_{pp}$  leads in many cases to inconsistent results for the single beta decays.

(b) As seen from Figs. 8–10, the bulk of the contributions to the  $0\nu\beta\beta$ -decay matrix element, i.e., the contributions coming from all multipoles except  $1^+$ , remains practically unaffected by the changes in  $g_{pp}$ .

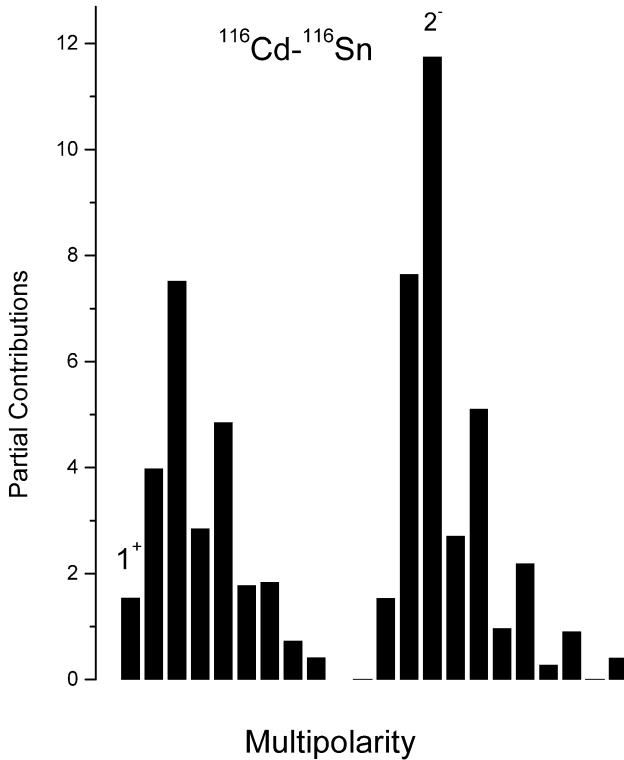


Fig. 14. Multipole decomposition of the matrix element  $M_{GT}^{(0\nu)}$  for the decay of  $^{116}\text{Cd}$ . The values shown in the figure have been obtained with  $g_{pp} = 1.55$ .

(c) The contribution of the  $1^+$  states, which represents at most 10 percent of the total value of the  $0\nu\beta\beta$ -decay matrix element, varies strongly as a function of  $g_{pp}$ , like for the case of  $2\nu\beta\beta$  decays, but this is the only significant change observed in the multipole decomposition of the total matrix element.

(d) The largest contributions to the  $0\nu\beta\beta$ -decay matrix element are coming from the higher multipoles, especially from the  $2^-$  multipole.

These results support the notion that the procedure advanced in [14] is not that selective of proper values of  $g_{pp}$  as it was emphasized in that paper.

Finally, our conclusions, which are based on the results of realistic calculations, may be compared with the ones of Ref. [31], where the validity of the procedure of [14] is analyzed in the framework of a solvable Hamiltonian. In their conclusions the authors of [31] pointed out to the fact that “the procedure of [14] to eliminate model-space dependence in the QRPA helps but does not work as well in their model as in realistic calculations”. The results of our analysis point to difficulties also in realistic calculations.

## Acknowledgements

This work has been partially supported by the National Research Council (CONICET) of Argentina and by the Academy of Finland under the Finnish Centre of Excellence Programme 2000–2005 (Project No. 44875, Nuclear and Condensed Matter Programme at JYFL). One of the authors (O.C.) gratefully thanks the warm hospitality extended to him at the Department of Physics of the University of Jyväskylä, Finland.

## References

- [1] SNO Collaboration, Q.R. Ahmad, et al., *Phys. Rev. Lett.* 89 (2002) 011301;  
SNO Collaboration, Q.R. Ahmad, et al., *Phys. Rev. Lett.* 89 (2002) 011302;  
Super-Kamiokande Collaboration, S. Fukuda, et al., *Phys. Rev. Lett.* 86 (2001) 5651;  
KamLAND Collaboration, K. Eguchi, et al., *Phys. Rev. Lett.* 90 (2003) 021802;  
M. Appollonio, et al., *Phys. Lett. B* 466 (1999) 415;  
C.L. Bennet, et al., *astro-ph/0302207*.
- [2] S. Pascoli, S.T. Petcov, *Phys. Lett. B* 580 (2004) 280.
- [3] S.R. Elliot, P. Vogel, *Annu. Rev. Nucl. Part. Sci.* 52 (2002) 115;  
S.R. Elliot, J. Engel, *J. Phys. G* 30 (2004) R183.
- [4] F. Simkovic, A. Faessler, *Prog. Part. Nucl. Phys.* 48 (2002) 201.
- [5] M. Moe, P. Vogel, *Annu. Rev. Nucl. Part. Sci.* 44 (1994) 247.
- [6] J. Suhonen, O. Civitarese, *Phys. Rep.* 300 (1998) 123.
- [7] P. Vogel, M. Zirnbauer, *Phys. Rev. Lett.* 57 (1986) 3148.
- [8] O. Civitarese, A. Faessler, T. Tomoda, *Phys. Lett. B* 194 (1987) 11.
- [9] J. Suhonen, O. Civitarese, *Phys. Lett. B* 497 (2001) 221.
- [10] J. Suhonen, *Nucl. Phys. A* 700 (2002) 649.
- [11] J. Suhonen, O. Civitarese, *Phys. Rev. C* 49 (1994) 3055.
- [12] M. Aunola, J. Suhonen, *Nucl. Phys. A* 602 (1996) 133;  
M. Aunola, J. Suhonen, *Nucl. Phys. A* 643 (1998) 207.
- [13] J. Suhonen, *Phys. Lett. B* 607 (2005) 87.
- [14] V.A. Rodin, A. Faessler, F. Simkovic, P. Vogel, *Phys. Rev. C* 68 (2003) 044302.
- [15] E. Caurier, F. Nowacki, A. Poves, J. Retamosa, *Nucl. Phys.* 654 (1999) 973c–976c;  
E. Caurier, F. Nowacki, A.P. Zuker, G. Martinez-Pinedo, A. Poves, J. Retamosa, *Nucl. Phys.* 654 (1999) 747c–758c.
- [16] E. Caurier, G. Martinez-Pinedo, *Nucl. Phys. A* 704 (2002) 60.
- [17] J. Toivanen, J. Suhonen, *Phys. Rev. Lett.* 75 (1995) 410.
- [18] O. Civitarese, J. Suhonen, *Nucl. Phys. A* 653 (1999) 321.
- [19] M. Doi, T. Kotani, E. Takasugi, *Prog. Theor. Phys. Suppl.* 83 (1985) 1.
- [20] O. Civitarese, J. Suhonen, *Nucl. Phys. A* 729 (2003) 867.
- [21] S.M. Bilenky, A. Faessler, F. Simkovic, *Phys. Rev. D* 70 (2004) 033003.
- [22] A. Faessler, F. Simkovic, *J. Phys. G* 24 (1998) 2139.
- [23] J. Suhonen, S.B. Khadkikar, A. Faessler, *Nucl. Phys. A* 529 (1991) 727.
- [24] A. Bohr, B.R. Mottelson, *Nuclear Structure*, vol. I, Benjamin, New York, 1969.
- [25] J. Suhonen, T. Taigel, A. Faessler, *Nucl. Phys. A* 486 (1988) 91.
- [26] A.S. Barabash, *Czech J. Phys.* 52 (2002) 567.
- [27] V.I. Tretyak, Yu.G. Zdesenko, *At. Data Nucl. Data Tables* 80 (2002) 83;  
V.I. Tretyak, Yu.G. Zdesenko, *At. Data Nucl. Data Tables* 61 (1995) 43;  
E.A. Danevich, et al., *Phys. At. Nucl.* 59 (1996) 1.
- [28] O. Civitarese, J. Suhonen, *Phys. Lett. B*, submitted for publication.
- [29] M. Hirsch, K. Muto, T. Oda, H.V. Klapdor-Kleingrothaus, *Z. Phys. A* 347 (1994) 151.
- [30] A. Griffiths, P. Vogel, *Phys. Rev. C* 46 (1992) 181.
- [31] J. Engel, P. Vogel, *Phys. Rev. C* 69 (2004) 034304.